Reference Correlations for the Viscosity and Thermal Conductivity of *n*-Undecane

Cite as: J. Phys. Chem. Ref. Data **46**, 033103 (2017); https://doi.org/10.1063/1.4996885
Submitted: 19 July 2017 . Accepted: 31 August 2017 . Published Online: 26 September 2017

M. J. Assael, T. B. Papalas, and M. L. Huber

Reference Correlations for the Viscosity and Thermal Conductivity of *n*-Undecane

M. J. Assael and T. B. Papalas

Laboratory of Thermophysical Properties and Environmental Processes, Chemical Engineering Department, Aristotle University, Thessaloniki 54636, Greece

M. L. Huber[a)]

Applied Chemicals and Materials Division, National Institute of Standards and Technology, 325 Broadway, Boulder, Colorado 80305, USA

(Received 19 July 2017; accepted 31 August 2017; published online 26 September 2017)

This paper presents new, wide-ranging correlations for the viscosity and thermal conductivity of *n*-undecane based on critically evaluated experimental data. The correlations are designed to be used with a recently published equation of state that is valid from the triple point to 700 K, at pressures up to 500 MPa, with densities below 776.86 kg m^{-3}. The estimated uncertainty for the dilute-gas viscosity is 2.4%, and the estimated uncertainty for viscosity in the liquid phase for pressures up to 60 MPa over the temperature range 260 K–520 K is 5%. The estimated uncertainty is 3% for the thermal conductivity of the low-density gas and 3% for the liquid over the temperature range from 284 K to 677 K at pressures up to 400 MPa. Both correlations behave in a physically reasonable manner when extrapolated to the full range of the equation of state, but care should be taken when using the correlations outside of the validated range. The uncertainties will be larger outside of the validated range and also in the critical region. https://doi.org/10.1063/1.4996885

Key words: thermal conductivity; transport properties; *n*-undecane; viscosity.

CONTENTS

1. Introduction 2
2. Viscosity Methodology 2
   2.1. The viscosity dilute-gas limit and the initial-density dependence terms 4
   2.2. The viscosity residual term 4
3. Thermal Conductivity Methodology 6
   3.1. The thermal conductivity dilute-gas limit . 7
   3.2. The thermal conductivity residual term . . 8
   3.3. The thermal conductivity critical enhancement term 8
4. Recommended Values and Computer-Program Verification 10
   4.1. Recommended values 10
   4.2. Computer-program verification 10
5. Conclusions 10
6. References 11

List of Tables

1. Viscosity measurements of *n*-undecane 3
2. Coefficients c_i for Eq. (8) 5
3. Evaluation of the *n*-undecane viscosity correlation for the primary data 5
4. Evaluation of the *n*-undecane viscosity correlation for the secondary data 5
5. Thermal conductivity measurements of *n*-undecane 6
6. Coefficients of Eq. (15) for the residual thermal conductivity of *n*-undecane 8
7. Evaluation of the *n*-undecane thermal conductivity correlation for the primary data 9
8. Evaluation of the *n*-undecane thermal conductivity correlation for the secondary data 9
9. Viscosity and thermal conductivity values of *n*-undecane along the saturation line, calculated by the present scheme 10
10. Viscosity and thermal conductivity values of *n*-undecane at selected temperatures and pressures, calculated by the present scheme 10
11. Sample points for computer verification of the correlating equations 10

a)Author to whom correspondence should be addressed; electronic mail: marcia.huber@nist.gov.

List of Figures

1. Temperature–pressure ranges of the primary experimental viscosity data for *n*-undecane 3
2. Temperature–density ranges of the primary experimental viscosity data for *n*-undecane 3
3. Percentage deviations of primary experimental data of *n*-undecane from the values calculated by the present model as a function of temperature 5
4. Percentage deviations of primary experimental data of *n*-undecane from the values calculated by the present model as a function of pressure . . . 5
5. Percentage deviations of primary experimental data of *n*-undecane from the values calculated by the present model as a function of density . . . 5
6. Viscosity of *n*-undecane as a function of temperature for different pressures 6
7. Temperature–pressure range of the primary experimental thermal conductivity data for *n*-undecane 6
8. Temperature–density range of the primary experimental thermal conductivity data for *n*-undecane 7
9. Primary dilute-gas thermal-conductivity of *n*-undecane as a function of temperature 8
10. Percentage deviations of the primary dilute-gas thermal-conductivity measurements of *n*-undecane from Eq. (14) as a function of temperature. 8
11. Percentage deviations of primary thermal conductivity experimental data of *n*-undecane from the values calculated by the present model as a function of temperature 9
12. Percentage deviations of primary thermal conductivity experimental data of *n*-undecane from the values calculated by the present model as a function of pressure 9
13. Percentage deviations of primary thermal conductivity experimental data of *n*-undecane from the values calculated by the present model as a function of density 9
14. Thermal conductivity of *n*-undecane as a function of temperature for selected pressures 10
15. Thermal conductivity of *n*-undecane as a function of density for selected temperatures 10

1. Introduction

In a series of recent papers, new reference correlations for the thermal conductivity of normal- and parahydrogen,[1] water,[2] SF_6,[3] carbon dioxide,[4] toluene,[5] benzene,[6] *n*-pentane and *iso*-pentane,[7] *n*-hexane,[8] cyclopentane,[7] cyclohexane,[9] *n*-heptane,[10] methanol,[11] ethanol,[12] ethene and propene,[13] and ortho-xylene, meta-xylene, para-xylene, and ethylbenzene,[14] as well as for the viscosity of water,[15] *n*-hexane,[16] *n*-heptane,[17] benzene,[18] and toluene,[19] covering a wide range of conditions of temperature and pressure, were reported. The work was also extended to refrigerants; thus reference correlations for the thermal conductivity of R245fa[20] and R161[21] and for the viscosity of R1234yf and R1234ze(E),[22] R245fa,[20] and R161[21] were reported. In this paper, the methodology adopted in the aforementioned papers is extended to developing new reference correlations for the viscosity and thermal conductivity of *n*-undecane. This fluid can serve as an example long-chain alkane that can be used to model natural gases with "heavies" in it and may also be useful as part of a surrogate model to use when modeling some hydrocarbon-based fuels (along with dodecane and hexadecane).

The goal of this work is to critically assess the available literature data and provide wide-ranging correlations for the viscosity and thermal conductivity of *n*-undecane that are valid over gas, liquid, and supercritical states and that incorporate densities provided by the 2011 Helmholtz equation of state (EOS) of Aleksandrov *et al.*[23]

The analysis that will be described will be applied to the best available experimental data for the viscosity and thermal conductivity. Thus, a prerequisite to the analysis is a critical assessment of the experimental data. For this purpose, two categories of experimental data are defined: primary data, employed in the development of the correlation, and secondary data, used simply for comparison purposes. According to the recommendation adopted by the Subcommittee on Transport Properties (now known as The International Association for Transport Properties) of the International Union of Pure and Applied Chemistry, the primary data are identified by a well-established set of criteria.[24] These criteria have been successfully employed to establish standard reference values for the viscosity and thermal conductivity of fluids over wide ranges of conditions, with uncertainties in the range of 1%. However, in many cases, such a narrow definition unacceptably limits the range of the data representation. Consequently, within the primary data set, it is also necessary to include results that extend over a wide range of conditions, albeit with a poorer accuracy, provided they are consistent with other more accurate data or with theory. In all cases, the accuracy claimed for the final recommended data must reflect the estimated uncertainty in the primary information.

2. Viscosity Methodology

The viscosity η can be expressed[16–20,22] as the sum of four independent contributions, as

$$\eta(\rho,T) = \eta_0(T) + \eta_1(T)\rho + \Delta\eta(\rho,T) + \Delta\eta_c(\rho,T), \quad (1)$$

where ρ is the molar density, T is the absolute temperature, and the first term, $\eta_0(T) = \eta(0, T)$, is the contribution to the viscosity in the dilute-gas limit, where only two-body molecular interactions occur. The linear-in-density term, $\eta_1(T)\,\rho$, known as the initial density dependence term, can be

TABLE 1. Viscosity measurements of *n*-undecane

First author	Year of publication	Technique employed[a]	Purity (%)	Uncertainty (%)	No. of data	Temperature range (K)	Pressure range (MPa)
Primary data							
Iglesias-Silva[28]	2016	RBALL	99.0	0.5	17	283–363	0.1
Zhang[29]	2010	UCAP	99.0	0.8	1	298	0.1
Wu[30]	1998	CAP	99.0	0.1	4	293–313	0.1
Assael[31]	1991	VBW	99.0	0.5	28	303–333	0.100–62
Bauer[32]	1984	UCAP	99.5	0.04	2	293–298	0.1
Guseinov[33]	1973	CAP	–	2.4	87	292–520	0.245–49
Doolittle[34]	1951	UCAP	Purified	0.09	5	262–473	0.1
Rastorguev[35]	1971	CAP	98.5	1.2	41	302–513	0.098–49
Secondary data							
Shepard[36]	1931	CAP	–	0.5	1	298	0.1
Bingham[37]	1930	CAP	–	–	8	273–373	0.1

[a]CAP, Capillary; RBALL, Rolling Ball; UCAP, Ubbelohde Capillary; VBW, Vibrating Wire.

separately established with the development of the Rainwater-Friend theory[25–27] for the transport properties of moderately dense gases. The critical enhancement term, $\Delta\eta_c(\rho, T)$, arises from the long-range density fluctuations that occur in a fluid near its critical point, which contribute to divergence of the viscosity at the critical point. Finally, the term $\Delta\eta(\rho, T)$, the residual term, represents the contribution of all other effects to the viscosity of the fluid at elevated densities including many-body collisions, molecular-velocity correlations, and collisional transfer.

The identification of these four separate contributions to the viscosity and to transport properties in general is useful because it is possible, to some extent, to treat $\eta_0(T)$, $\eta_1(T)$, and $\Delta\eta_c(\rho, T)$ theoretically. In addition, it is possible to derive information about both $\eta_0(T)$ and $\eta_1(T)$ from experiment. In contrast, there is little theoretical guidance concerning the residual contribution, $\Delta\eta(\rho, T)$, and therefore its evaluation is based entirely on an empirical equation obtained by fitting experimental data.

Table 1 summarizes, to the best of our knowledge, the experimental measurements[28–36] of the viscosity of *n*-undecane reported in the literature. The measurements of Assael and Papadaki,[31] extended up to 60 MPa pressure, were performed in a vibrating-wire instrument backed by a full theoretical model, with an uncertainty of 0.5%. Measurements from this group have successfully been employed in previous reference correlations,[16–19] and thus this set was considered as primary data. The measurements of Bauer and Meerlender[32] were performed in an Ubbelohde capillary with a very low uncertainty, 0.04%. These were also considered as primary data, as measurements from this group have previously also been employed in other reference correlations.[16,18,19] Capillary measurements were also performed by Zhang *et al.*,[29] Wu *et al.*,[30] and Doolittle and Peterson,[34] with corresponding uncertainties of 0.8%, 0.1%, and 0.01%; these were also considered part of the primary data set. In addition to the high-pressure measurements of Assael and Papadaki,[31] Guseinov and Naziev[33] and Rastorguev and Keramidi[35] employed capillary viscometers to measure the viscosity of *n*-undecane up to 49 MPa with corresponding uncertainties of 2.4% and 1.2%, respectively. These measurements were also considered part of the primary data set. Finally, the measurements of Iglesias-Silva *et al.*,[28] performed in a rolling-ball viscometer with an uncertainty of 0.5%, were considered as primary data. The rest of the measurements were considered as secondary data.

Figures 1 and 2 show the ranges of the primary measurements outlined in Table 1, and the phase boundary may be seen as well. The development of the correlation requires densities; Aleksandrov *et al.*[23] in 2011 published an accurate, wide-ranging equation of Helmholtz-energy equation of state that is valid from the triple point up to 700 K and 500 MPa, with densities below 776.86 kg m^{-3}, with an uncertainty in saturated liquid density of 0.05%–0.15%; saturated vapor density, 0.2%–0.4% at temperatures below 500 K, while at higher temperatures, the uncertainty reaches 3%–4%; liquid-phase density, 0.1%–0.3%; gas-phase density, 0.20%–0.35%;

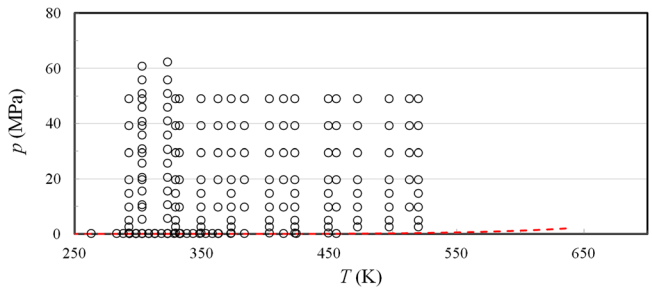

FIG. 1. Temperature–pressure ranges of the primary experimental viscosity data for *n*-undecane. The dashed line indicates the saturation curve.

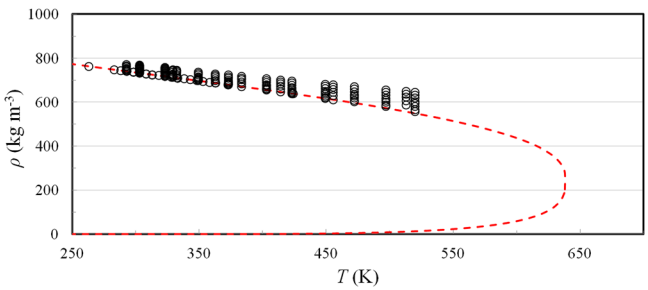

FIG. 2. Temperature–density ranges of the primary experimental viscosity data for *n*-undecane. The dashed curve indicates the saturation curve.

and heat capacities, 0.4%–0.8%. We also adopt the values for the critical point from their EOS; the critical temperature, T_c, and the critical density, ρ_c, are 638.8 K and 236.7914 kg m^{-3}, respectively.[23] The triple-point temperature resulting from critically evaluating available literature data is 247.606 K.[38]

2.1. The viscosity dilute-gas limit and the initial-density dependence terms

As indicated in Table 1, along with Figs. 1 and 2, there are no vapor-phase viscosity measurements for *n*-undecane, and the dilute-gas limit viscosity, $\eta_0(T)$, was calculated with a theoretical model. In 2016, Riesco and Vesovic[39] published a theoretical scheme for the calculation of the dilute-gas limit viscosity of *n*-alkanes up to *n*-$C_{40}H_{82}$ with an uncertainty of ±2.4%. According to their scheme,[39] the viscosity in the zero-density limit, $\eta_0(T)$ in μPa s, was represented by means of a standard relationship in kinetic theory,[40] which in practical engineering form is given by

$$\eta_0(T) = 0.083\,867\sqrt{MT}\,\frac{f_\eta}{\Omega_\eta}, \tag{2}$$

where Ω_η is the viscosity collision integral, M is the molar mass, and f_η is the higher-order correction factor, usually within a few percent of unity,[39] both given as

$$\Omega_\eta = \pi\sigma^2\Omega^*_\eta, \tag{3}$$

$$\begin{aligned}\Omega^*_\eta = {} & 1.161\,45T^{*-0.14874} + 0.524\,87\exp(-0.7732T^*) \\ & + 2.161\,78\exp(-2.437\,87T^*) \\ & - 6.435\times10^{-4}T^{*0.14874}\sin\left(18.0323T^{*-0.76830} - 7.273\,71\right)\end{aligned} \tag{4}$$

and

$$f_\eta = 1 + \frac{3}{49}(4E^* - 3.5)^2, \tag{5}$$

$$\begin{aligned}E^* = {} & [1.115\,21T^{*-0.14796} + 0.448\,44\exp(-0.995\,48T^*) \\ & + 2.300\,09\exp(-3.060\,31T^*) \\ & + 4.565\times10^{-4}T^{*-0.14796} \\ & \times\sin\left(38.5868T^{*-0.69403} - 2.563\,75\right)]/\Omega^*_\eta\end{aligned} \tag{6}$$

where $T^* = T/\varepsilon$ is the reduced temperature and ε (K) and σ (nm) are the energy and length scaling parameters, respectively. These two parameters were obtained with the method of Riesco and Vesovic[39] as ε = 445.75 K and σ = 0.7815 nm.

Equations (2)–(6) present a consistent scheme for the correlation of the dilute-gas limit viscosity, $\eta_0(T)$. The values of the dilute-gas limit viscosity, $\eta_0(T)$ in μPa s, obtained by the scheme of Eqs. (2)–(6), were fitted as a function of the reduced temperature $T_r = T/T_c$ for ease of use to the following equation:

$$\eta_0(T) = \frac{0.773\,488 - 1.536\,41T_r + 19.9976T_r^2 - 7.581\,48T_r^3 + 2.151\,43T_r^4 - 0.261\,065T_r^5}{0.313\,626 + T_r}. \tag{7}$$

Values calculated by Eq. (7) do not deviate from the values calculated by the scheme of Eqs. (2)–(6) by more than 0.1% over the temperature range from 248 K to 1000 K. Equation (7) is hence employed in the calculations that will follow.

In several past studies,[16–21] we have used the Rainwater-Friend theory[25,26] to predict values for the initial-density dependence term $\eta_1(T)\rho$. Due to the large size and non-spherical shape of *n*-undecane, we have not used this method to calculate the initial density dependence separately and instead it will be included in the empirical residual term in Eq. (1). In addition, due to the lack of any data in the critical region, and the fact that the critical enhancement in viscosity is confined to a small region and becomes relevant only at temperatures and densities very close to the critical point, we will neglect this term as we have done in previous studies.[16–21]

2.2. The viscosity residual term

As stated in Sec. 2, the residual viscosity term, $\Delta\eta(\rho, T)$, represents the contribution of all other effects to the viscosity of the fluid at elevated densities including many-body collisions, molecular-velocity correlations, and collisional transfer. Because there is little theoretical guidance concerning this term, its evaluation here is based entirely on experimentally obtained data.

The procedure adopted during this analysis used symbolic regression software[41] to fit all the primary data to the residual viscosity. Symbolic regression is a type of genetic programming that allows the exploration of arbitrary functional forms to regress data. The functional form is obtained by using a set of operators, parameters, and variables as building blocks. Most recently, this method has been used to obtain correlations for the viscosity of *n*-hexane,[16] *n*-heptane,[17] R1234yf and R1234ze(E),[22] and R245fa.[20] In the present work, we restricted the operators to the set (+,−,*,/) and the operands (constant, T_r, ρ_r), with $T_r = T/T_c$ and $\rho_r = \rho/\rho_c$. In addition, we adopted a form suggested from the hard-sphere model employed by Assael *et al.*,[42] $\Delta\eta(\rho_r,T_r) = (\rho_r^{2/3}T_r^{1/2})F(\rho_r,T_r)$, where the symbolic regression method was used to determine the functional form for $F(\rho_r,T_r)$. For this task, the dilute-gas limit was calculated for each experimental point, employing Eq. (7), and subtracted from the experimental viscosity to obtain the residual term. The density values employed were obtained by the equation of state of Aleksandrov *et al.*[23] The final equation obtained was

$$\Delta\eta(\rho,T)=\left(\rho_r^{2/3}T_r^{1/2}\right)\left\{\frac{c_0}{c_1+c_2T_r+\rho_r^2+T_r^2+c_3\rho_rT_r+c_4\rho_r}\right\}. \quad (8)$$

Coefficients c_i are given in Table 2, and $\Delta\eta$ is in μPa s.

Table 3 summarizes comparisons of the primary data with the correlation. We have defined the percent deviation as PCTDEV = 100*(η_{exp} − η_{fit})/η_{fit}, where η_{exp} is the experimental value of the viscosity and η_{fit} is the value calculated from the correlation. Thus, the average absolute percent deviation (AAD) is found with the expression AAD = ($\sum|$PCTDEV$|$)/n, where the summation is over all n points, the bias percent is found with the expression BIAS = ($\sum$PCTDEV)/n. The AAD of the fit is 2.04%, and its bias is 0.90%. We estimate the uncertainty for viscosity in the liquid phase for pressures up to 60 MPa over the temperature range 260 K–520 K to be 5.0% (at a 95% confidence level). Outside of this region, the deviations may be larger. As mentioned earlier, the zero-density values have an estimated uncertainty of 2.4%.

Figure 3 shows the percentage deviations of all primary viscosity data from the values calculated by Eqs. (7) and (8), as a function of temperature, while Figs. 4 and 5 show the same deviations but as a function of the pressure and the density. Table 4 shows the AAD and the bias for the secondary data. Finally, Fig. 6 shows a plot of the viscosity of *n*-undecane as a function of the temperature for different

TABLE 2. Coefficients c_i for Eq. (8)

i	c_i
0	256.663 94
1	10.351 826
2	6.497 773 6
3	−1.968 383
4	−6.453 049 2

TABLE 3. Evaluation of the *n*-undecane viscosity correlation for the primary data

First author	Year of publication	AAD (%)	BIAS (%)
Iglesias-Silva[28]	2016	2.49	−2.49
Zhang[29]	2010	1.92	1.92
Wu[30]	1998	0.40	0.03
Assael[31]	1991	0.70	−0.34
Bauer[32]	1984	0.42	0.42
Guseinov[33]	1973	2.41	1.90
Doolittle[34]	1951	1.65	1.29
Rastorguev[35]	1971	2.21	1.10
Entire data set		2.04	0.90

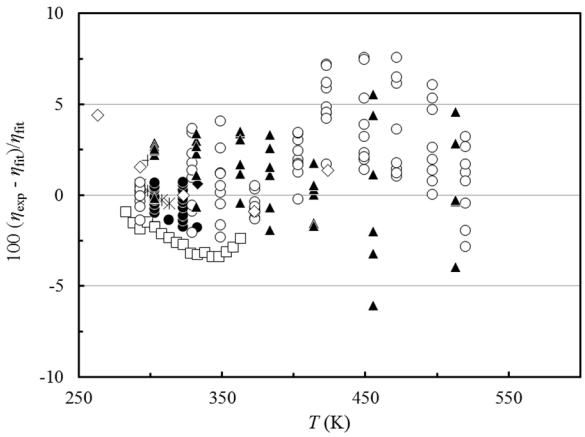

FIG. 3. Percentage deviations of primary experimental data of *n*-undecane from the values calculated by the present model as a function of temperature. Iglesias-Silva *et al.*[28] (□), Zhang *et al.*[29] (+), Wu *et al.*[30] (⁎), Assael and Papadaki[31] (●), Bauer and Meerlender[32] (◆), Guseinov and Naziev[33] (○), Rastorguev and Keramidi[35] (▲), and Doolittle and Peterson[34] (◇).

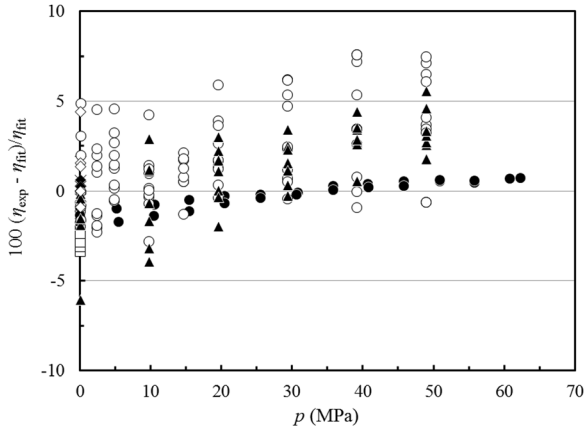

FIG. 4. Percentage deviations of primary experimental data of *n*-undecane from the values calculated by the present model as a function of pressure. Iglesias-Silva *et al.*[28] (□), Zhang *et al.*[29] (+), Wu *et al.*[30] (⁎), Assael and Papadaki[31] (●), Bauer and Meerlender[32] (◆), Guseinov and Naziev[33] (○), Rastorguev and Keramidi[35] (▲), and Doolittle and Peterson[34] (◇).

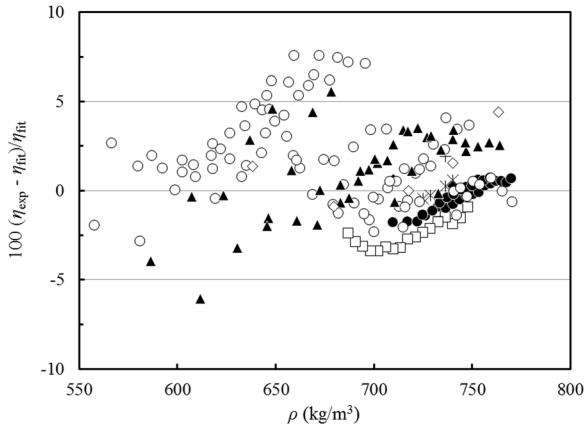

FIG. 5. Percentage deviations of primary experimental data of *n*-undecane from the values calculated by the present model as a function of density. Iglesias-Silva *et al.*[28] (□), Zhang *et al.*[29] (+), Wu *et al.*[30] (⁎), Assael and Papadaki[31] (●), Bauer and Meerlender[32] (◆), Guseinov and Naziev[33] (○), Rastorguev and Keramidi[35] (▲), and Doolittle and Peterson[34] (◇).

TABLE 4. Evaluation of the *n*-undecane viscosity correlation for the secondary data

First author	Year of publication	AAD (%)	BIAS (%)
Shepard[36]	1931	0.24	0.24
Bingham[37]	1930	1.40	−0.38

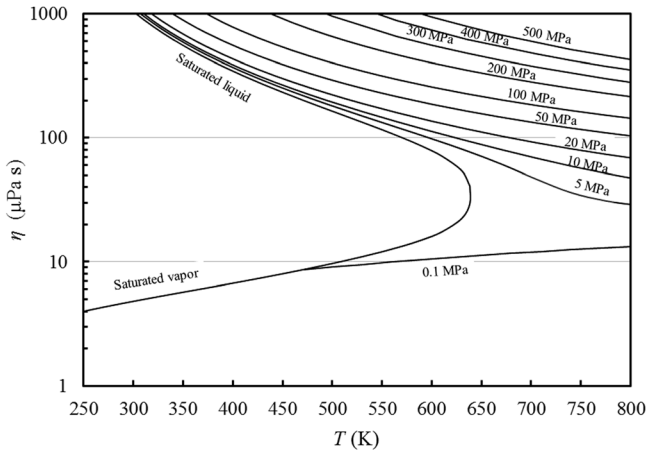

FIG. 6. Viscosity of *n*-undecane as a function of temperature for different pressures.

pressures. The plot demonstrates the extrapolation behavior at pressures higher than 60 MPa and at temperatures that exceed the 700 K limit of the equation of state.

3. Thermal Conductivity Methodology

In a very similar fashion to that described for the viscosity in Sec. 2, the thermal conductivity λ is expressed as the sum of three independent contributions, as

$$\lambda(\rho,T) = \lambda_o(T) + \Delta\lambda(\rho,T) + \Delta\lambda_c(\rho,T), \qquad (9)$$

where ρ is the density, T is the temperature, and the first term, $\lambda_o(T) = \lambda(0,T)$, is the contribution to the thermal conductivity in the dilute-gas limit, where only two-body molecular interactions occur. The final term, $\Delta\lambda_c(\rho,T)$, the critical enhancement, arises from the long-range density fluctuations that occur in a fluid near its critical point, which contribute to divergence of the thermal conductivity at the critical point. Finally, the term $\Delta\lambda(\rho,T)$, the residual property, represents the contribution of all other effects to the thermal conductivity of the fluid at elevated densities.

Table 5 summarizes, to the best of our knowledge, the experimental measurements[43–53] of the thermal conductivity of *n*-undecane reported in the literature. The measurements of Wada *et al.*,[43] Calado *et al.*,[44] and Menashe and Wakeham[45] were performed in absolute transient hot-wire instruments employing a complete theoretical model that operated with uncertainties of 1%, 1.5%, and 0.7%, respectively. Furthermore, measurements from these three groups have already been successfully employed in previous correlations as primary data (Wada *et al.*[43] in Refs. 5 and 10, Calado *et al.*[44] in Refs. 5, 8, and 10, and Menashe and Wakeham[45] in Refs. 5, 6, 8, and 10). Hence, these three sets were considered as primary data. Mukhamedzyanov *et al.*[49] also employed a transient hot-wire instrument with an uncertainty of 1%. This set was also considered as primary data, as measurements from this group have already been successfully employed in previous correlations[7,8,11,12] as such. A hot-wire instrument was employed by Mustafaev[46] and Mustafaev[47] for measurements in the vapor and liquid phases with an uncertainty of 2%. As measurements from this investigator have previously been successfully employed in other reference correlations,[14] these sets were also considered as primary data. Finally the measurements of Tarzimanov and Mashirov,[48] performed in a hot-wire instrument with an uncertainty of 4%, were also included in the primary data set, as they were in the vapor phase and have also been included in previous reference correlations.[6,11–13] The remaining sets were considered as secondary.

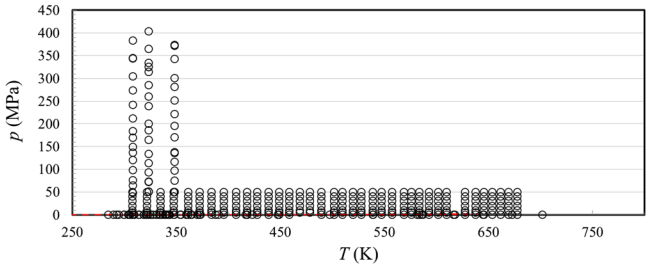

FIG. 7. Temperature–pressure range of the primary experimental thermal conductivity data for *n*-undecane. The dashed line indicates the saturation curve.

TABLE 5. Thermal conductivity measurements of *n*-undecane

First author	Year of publication	Technique employed[a]	Purity (%)	Uncertainty (%)	No. of data	Temperature range (K)	Pressure range (MPa)
Primary data							
Wada[43]	1985	THW	99.00	1.0	8	292–363	0.1
Calado[44]	1983	THW	99.00	1.5	39	284–373	0.000 02–0.0045
Menashe[45]	1982	THW	99.50	0.7	51	308–348	47.4–403
Mustafeav[46,b]	1974	CAL	–	2	22	489–677	0.1
Mustafeav[47]	1972	DCAL	–	2	231	307–677	0.1–50
Tarzimanov[48,b]	1970	HW	99.97	4	9	497–702	0.098
Mukhamedzyanov[49]	1963	THW	–	1.0	12	305–447	0.1
Secondary data							
Naziev[50]	1973	CC	–	2.0	94	313–613	0.1–14
Powell[51]	1972	ThComp	–	3.0	1	303	0.000 08
Abas-Zade[52]	1966	CAL	–	2.5	30	293–395	0.1–40
Akhmedov[53]	1963	CAL	–	1.4	2	293–323	0.1

[a]CAL, Calorimeter; CC, Concentric Cylinders; DCAL, Double Calorimeter; HW, Hot Wire; ThComp, Thermal Comparator; THW, Transient Hot Wire.
[b]Include vapor-phase measurements.

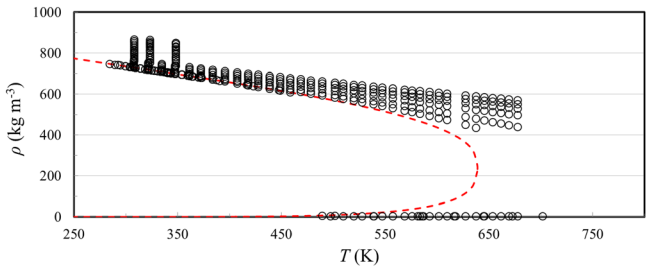

FIG. 8. Temperature–density range of the primary experimental thermal conductivity data for *n*-undecane. The dashed curve indicates the saturation curve.

Figures 7 and 8 show the range of the primary measurements outlined in Table 5, along with the saturation curve. The development of the correlation requires accurate values for the density, and as was done with the viscosity correlation, we use the EOS of Aleksandrov *et al.*[23] to provide densities.

3.1. The thermal conductivity dilute-gas limit

In order to be able to extrapolate the temperature range of the measurements, a theoretically based scheme was used to correlate the dilute-gas limit thermal conductivity, $\lambda_o(T)$, over a wide temperature range. The traditional kinetic approach for thermal conductivity results in an expression involving three generalized cross sections.[54,55] However, it is possible to derive an equivalent kinetic theory expression for thermal conductivity by making use of the approach of Thijsse *et al.*[56] and Millat *et al.*,[57] where one considers expansion in terms of total energy, rather than separating translational from internal energy as is done traditionally. In this case, the dilute-gas limit thermal conductivity, $\lambda_o(T)$ (mW m^{-1} K^{-1}), of a polyatomic gas can be shown to be inversely proportional to a single generalized cross section,[54–57] $S(10E)$ (nm^2), as

$$\lambda_o(T) = 1000\,\frac{5k_B^2(1+r^2)T}{2m\langle\nu\rangle_o S(10E)}\,f_\lambda, \tag{10}$$

where k_B is the Boltzmann constant (1.380 648 52 × 10^{-23} J K^{-1}), T (K) is the absolute temperature, f_λ (−) is the dimensionless higher-order correction factor, m (kg) is the molecular mass of *n*-undecane, and $\langle\nu\rangle_o = 4\sqrt{k_BT/\pi m}$ (m/s) is the average relative thermal speed. The dimensionless quantity r^2 is defined by $r^2 = 2C^o_{int}/5k_B$, where C^o_{int} is the contribution of both the rotational, C^o_{rot}, and the vibrational, C^o_{vib}, degrees of freedom to the isochoric ideal-gas heat capacity C^o_v.

The recent classical trajectory calculations[58–60] confirm that, for most molecules studied, the higher-order thermal-conductivity correction factor f_λ is near unity. One can take advantage of this finding to define the effective generalized cross section S_λ (=$S(10E)/f_\lambda$) (nm^2) and rewrite Eq. (10) for the dilute-gas limit thermal conductivity of *n*-undecane, $\lambda_o(T)$ (mW m^{-1} K^{-1}), as

$$\lambda_0(T) = 0.044\,619\,5\,\frac{(C^o_p/k_B)\sqrt{T}}{S_\lambda}. \tag{11}$$

The ideal-gas isobaric heat capacity per molecule, C^o_p (=C^o_{int} + 2.5k_B) in (J/K), can be obtained from Aleksandrov *et al.*[23] as

$$\frac{C^o_p}{k_B} = -1\,158\,848T^{-2} + 20\,321.8T^{-1} - 119.4274 + 0.428\,421\,5T - 4.157\,728\times10^{-4}T^2 + 1.618\,28\times10^{-7}T^3. \tag{12}$$

It has been previously noted,[57] and recently confirmed[55] for smaller molecules, that the cross section $S(10E)$ exhibits a nearly linear dependence on the inverse temperature. Hence, in order to develop the correlation, we fitted the effective cross section S_λ (nm^2), obtained from the only two low-density primary data sets shown in Table 5 (Tarzimanov and Mashirov[48] and Mustafaev[46]) by means of Eqs. (11) and (12), as a function of the inverse temperature, as

$$S_\lambda = 0.2637 + \frac{787.45}{T}. \tag{13}$$

Equations (11)–(13) form a consistent set of equations for the calculation of the dilute-gas limit thermal conductivity of *n*-undecane.

The values of the dilute-gas limit thermal conductivity, $\lambda_0(T)$ in mW m^{-1} K^{-1}, obtained by the scheme of Eqs. (11)–(13), were fitted as a function of the reduced temperature $T_r = T/T_c$ for ease of use to the following equation:

$$\lambda_0(T) = \frac{-37.3793 + 767.377\,T_r - 3043.34\,T_r^2 + 9056.43\,T_r^3 - 5922.11\,T_r^4 + 1527.46\,T_r^5}{27.743 + 27.1621\,T_r + T_r^2}. \tag{14}$$

Values calculated by Eq. (14) do not deviate from the values calculated by the scheme of Eqs. (11)–(13) by more than 0.03% over the temperature range from 248 K to 1000 K. Equation (14) is hence employed in the calculations that will follow.

Figure 9 shows the primary dilute-gas thermal-conductivity values of the selected investigators, and the values calculated by Eq. (14), as a function of temperature. In Fig. 10, percentage deviations of the primary dilute-gas thermal-conductivity values of *n*-undecane from Eq. (14) are shown. With the exception of one point, they all agree with the present correlation within a maximum deviation of 3%. Based on these measurements, the uncertainty of the correlation, at the 95% confidence level over the temperature range 489 K–702 K, is 3%. The correlation

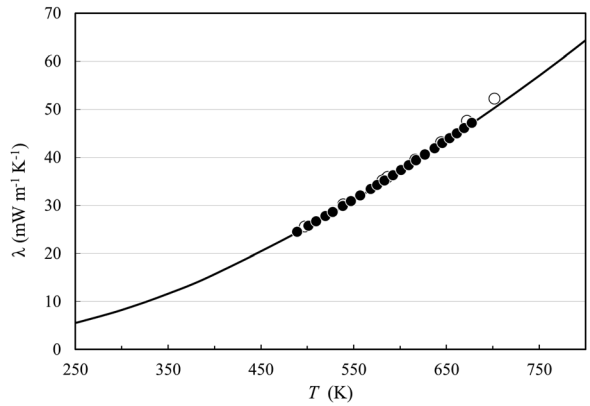

FIG. 9. Primary dilute-gas thermal-conductivity of *n*-undecane as a function of temperature. Mustafaev[46] (●), Tarzimanov and Mashirov[48] (o), and values calculated by Eq. (14).

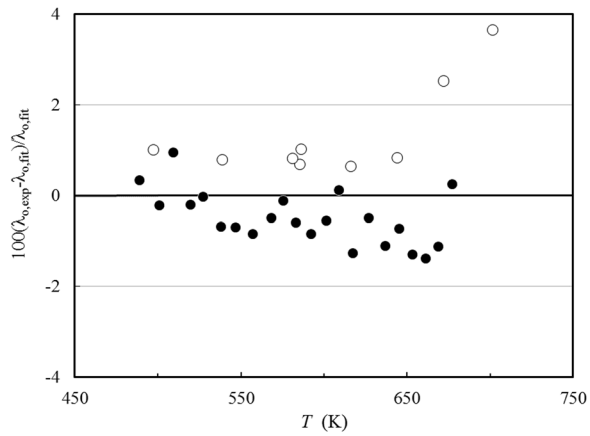

FIG. 10. Percentage deviations of the primary dilute-gas thermal-conductivity measurements of *n*-undecane from Eq. (14) as a function of temperature. Mustafaev[46] (●) and Tarzimanov and Mashirov[48] (o).

behaves in a physically reasonable manner over the entire range from the triple point to the highest temperature of the experimental data, 702 K; however, we anticipate that the uncertainty may be larger in the areas where data are unavailable and the correlation is extrapolated.

3.2. The thermal conductivity residual term

The thermal conductivities of pure fluids exhibit an enhancement over a large range of densities and temperatures around the critical point and become infinite at the critical point. This behavior can be described by models that produce a smooth crossover from the singular behavior of the thermal conductivity asymptotically close to the critical point to the residual values far away from the critical point.[61–63] The density-dependent terms for thermal conductivity can be grouped according to Eq. (9) as $[\Delta\lambda(\rho,T) + \Delta\lambda_c(\rho,T)]$. To assess the critical enhancement theoretically, we need to evaluate, in addition to the dilute-gas thermal conductivity, the residual thermal-conductivity contribution. The procedure adopted during this analysis used ODRPACK (Ref. 64) to fit all the primary data simultaneously to the residual thermal conductivity and the critical enhancement, while maintaining

TABLE 6. Coefficients of Eq. (15) for the residual thermal conductivity of *n*-undecane

i	$B_{1,i}$ (mW m^{-1} K^{-1})	$B_{2,i}$ (mW m^{-1} K^{-1})
1	$-0.573\,413 \times 10^{2}$	$0.646\,731 \times 10^{2}$
2	$0.815\,949 \times 10^{2}$	$-0.443\,965 \times 10^{2}$
3	$-0.354\,049 \times 10^{2}$	$0.153\,679 \times 10^{1}$
4	$0.831\,716 \times 10^{1}$	$0.320\,177 \times 10^{1}$
5	$-0.723\,814 \times 10^{0}$	$-0.308\,355 \times 10^{0}$

the values of the dilute-gas thermal-conductivity data already obtained. The density values employed were obtained by the equation of state of Aleksandrov *et al.*[23] The primary data were weighted in inverse proportion to the square of their uncertainty.

The residual thermal conductivity was represented with a polynomial in temperature and density,

$$\Delta\lambda(\rho,T) = \sum_{i=1}^{5}\left(B_{1,i} + B_{2,i}(T/T_c)\right)(\rho/\rho_c)^i. \qquad (15)$$

Coefficients $B_{1,i}$ and $B_{2,i}$ are shown in Table 6.

3.3. The thermal conductivity critical enhancement term

The theoretically based crossover model proposed by Olchowy and Sengers[61–63] is complex and requires solution of a quartic system of equations in terms of complex variables. A simplified crossover model has also been proposed by Olchowy and Sengers.[65] The critical enhancement of the thermal conductivity from this simplified model is given by

$$\Delta\lambda_c = \frac{\rho C_p R_D k_B T}{6\pi\overline{\eta}\xi}\left(\overline{\Omega} - \overline{\Omega}_0\right), \qquad (16)$$

with

$$\overline{\Omega} = \frac{2}{\pi}\left[\left(\frac{C_p - C_v}{C_p}\right)\arctan\left(\overline{q}_D\xi\right) + \frac{C_v}{C_p}\overline{q}_D\xi\right] \qquad (17)$$

and

$$\overline{\Omega}_0 = \frac{2}{\pi}\left[1 - \exp\left(-\frac{1}{\left(\overline{q}_D\xi\right)^{-1} + \left(\overline{q}_D\xi\rho_c/\rho\right)^2/3}\right)\right]. \qquad (18)$$

In Eqs. (16)–(18), $\overline{\eta}$ (Pa s) is the viscosity, and C_p and C_v (J kg^{-1} K^{-1}) are the isobaric and isochoric specific heat obtained from the equation of state. The correlation length ξ (m) is given by

$$\xi = \xi_0\left(\frac{p_c\rho}{\Gamma\rho_c^2}\right)^{\nu/\gamma}\left[\left.\frac{\partial\rho(T,\rho)}{\partial p}\right|_T - \left(\frac{T_{ref}}{T}\right)\left.\frac{\partial\rho\left(T_{ref},\rho\right)}{\partial p}\right|_T\right]^{\nu/\gamma}. \qquad (19)$$

As already mentioned, the coefficients $B_{1,i}$ and $B_{2,i}$ in Eq. (15) were fitted with ODRPACK (Ref. 64) to the primary

TABLE 7. Evaluation of the *n*-undecane thermal conductivity correlation for the primary data

First author	Year of publication	AAD (%)	BIAS (%)
Wada[43]	1985	1.08	0.53
Calado[44]	1983	1.02	−1.02
Menashe[45]	1982	0.18	0.08
Mustafaev[46]	1974	0.81	−0.58
Mustafaev[47]	1972	0.86	−0.59
Tarzimanov[48]	1970	1.18	1.18
Mukhamedzyanov[49]	1963	3.31	3.31
Entire data set		0.87	−0.35

data for the thermal conductivity of *n*-undecane. This crossover model requires the universal amplitude, $R_D = 1.02$ (−), the universal critical exponents, $\nu = 0.63$ and $\gamma = 1.239$, and the system-dependent amplitudes Γ and ξ_0. For this work, we adopted the values $\Gamma = 0.059$ (−), $\xi_0 = 0.267 \times 10^{-9}$ m, using the universal representation of the critical enhancement of the thermal conductivity by Perkins *et al.*[66] When there are sufficient experimental data available in the critical region, the remaining parameter $\overline{q}_D^{-1}$ may be found by regression. In this case, there are no critical-region data available, so we instead use the method of Perkins *et al.*[66] to estimate the effective cutoff wavelength $\overline{q}_D^{-1}$ (m). The estimated value is 8.66×10^{-10} m. The viscosity required for Eq. (16) was calculated with the correlation developed in Sec. 2. The reference temperature T_{ref}, far above the critical temperature where the critical enhancement is negligible, was calculated by $T_{ref} = (^3/_2)T_c$,[67] which for *n*-undecane is 958.2 K.

Table 7 summarizes comparisons of the primary data with the correlation. The AAD of the fit is 0.87%, and its bias is −0.35%. We estimate the uncertainty in thermal conductivity at a 95% confidence level to be 3% for the liquid phase over the temperature range 284 K–677 K at pressures up to 400 MPa.

Figure 11 shows the percentage deviations of all primary thermal conductivity data from the values calculated by Eqs. (9) and (14)–(19), as a function of temperature, while Figs. 12 and 13 show the same deviations but as a function of the pressure and the density. Table 8 shows the AAD and the bias for the secondary data. Figure 14 shows a plot of the thermal conductivity of *n*-undecane as a function of the temperature for different pressures. The plot demonstrates the smooth extrapolation behavior at conditions outside of the range of experimental data (above 700 K and 400 MPa). Finally, Fig. 15 shows the thermal conductivity of *n*-undecane as a function of the density for different temperatures, including the critical enhancement.

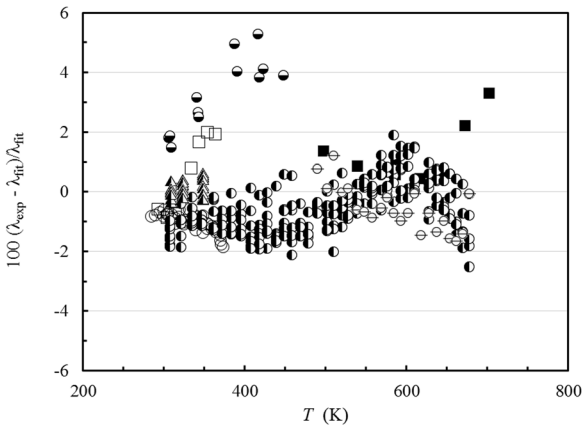

FIG. 11. Percentage deviations of primary thermal conductivity experimental data of *n*-undecane from the values calculated by the present model as a function of temperature. Calado[44] (○), Wada *et al.*[43] (□), Tarzimanov and Mashirov[48] (■), Mukhamedzyanov *et al.*[49] (◒), Mustafaev[47] (◐), Mustafaev[46] (⊖), and Menashe and Wakeham[45] (◭).

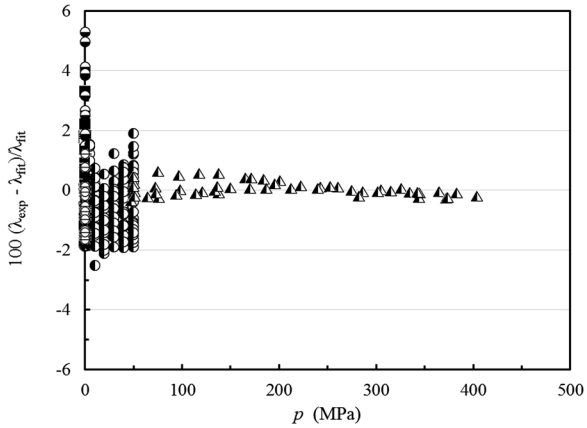

FIG. 12. Percentage deviations of primary thermal conductivity experimental data of *n*-undecane from the values calculated by the present model as a function of pressure. Calado[44] (○), Wada *et al.*[43] (□), Tarzimanov and Mashirov[48] (■), Mukhamedzyanov *et al.*[49] (◒), Mustafaev[47] (◐), Mustafaev[46] (⊖), and Menashe and Wakeham[45] (◭).

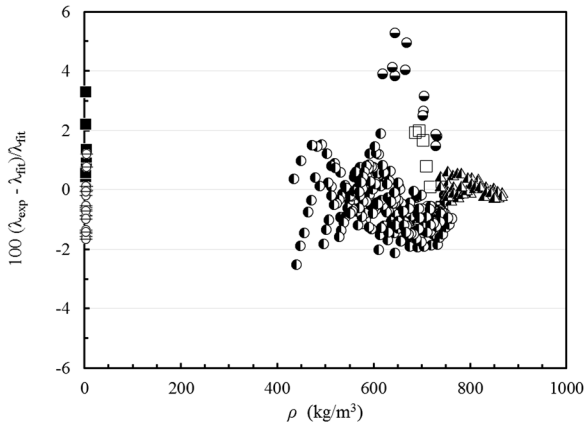

FIG. 13. Percentage deviations of primary thermal conductivity experimental data of *n*-undecane from the values calculated by the present model as a function of density. Calado[44] (○), Wada *et al.*[43] (□), Tarzimanov and Mashirov[48] (■), Mukhamedzyanov *et al.*[49] (◒), Mustafaev[47] (◐), Mustafaev[46] (⊖), and Menashe and Wakeham[45] (◭).

TABLE 8. Evaluation of the *n*-undecane thermal conductivity correlation for the secondary data

First author	Year of publication	AAD (%)	BIAS (%)
Naziev[50]	1973	6.06	5.36
Powell[51]	1972	4.46	4.46
Abas-Zade[52]	1966	3.35	3.35
Akhmedov[53]	1963	7.23	−7.23
Entire data set		5.43	4.70

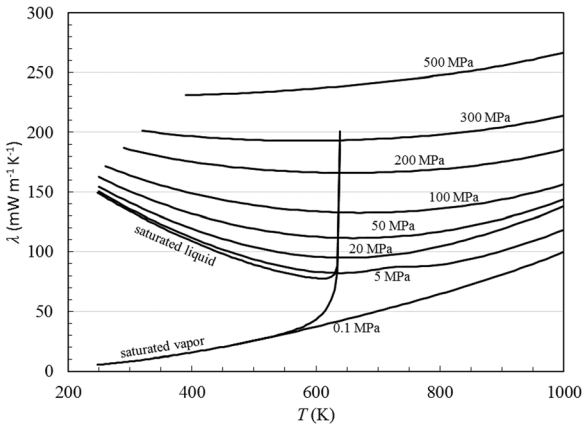

FIG. 14. Thermal conductivity of *n*-undecane as a function of temperature for selected pressures.

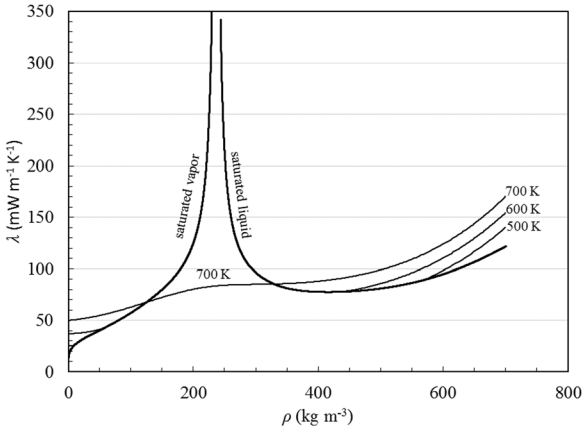

FIG. 15. Thermal conductivity of *n*-undecane as a function of density for selected temperatures.

4. Recommended Values and Computer-Program Verification

4.1. Recommended values

In Table 9, viscosity and thermal conductivity values are given along the saturated liquid line, calculated from the present proposed correlations between 300 and 600 K, while in Table 10, viscosity and thermal conductivity values are given for temperatures between 300 and 600 K at selected pressures. Saturation pressure and saturation density values for selected temperatures, as well as the density values for the selected temperature and pressure, are obtained from the equation of state of Aleksandrov *et al.*[23]

TABLE 10. Viscosity and thermal conductivity values of *n*-undecane at selected temperatures and pressures, calculated by the present scheme

p (MPa)	T (K)	ρ (kg m^{-3})	η (μPa s)	λ (mW m^{-1} K^{-1})
10	300	742.37	1168.8	137.7
	350	706.72	619.6	125.3
	400	671.21	389.5	114.4
	450	634.96	268.2	105.1
	500	597.18	195.1	97.5
	550	557.06	146.9	91.8
	600	513.80	113.1	88.2
25	300	752.25	1366.2	142.9
	350	719.42	716.6	131.5
	400	687.53	452.0	121.7
	450	656.08	315.1	113.5
	500	624.74	233.8	106.9
	550	593.38	181.3	102.1
	600	562.02	145.2	99.2
50	300	766.49	1744.2	150.6
	350	736.95	889.3	140.5
	400	708.95	557.2	132.0
	450	682.06	389.7	125.0
	500	656.08	291.8	119.4
	550	630.88	229.2	115.4
	600	606.47	186.5	112.8

TABLE 11. Sample points for computer verification of the correlating equations

T (K)	ρ (kg m^{-3})	η (μPa s)	λ (mW m^{-1} K^{-1})
550	0	8.935	31.153
550	10	10.702	31.211
550	600	188.68	104.28
635	0	10.252	41.522
635	325	49.077	69.829[a]
635	325	49.077	78.669

[a]Calculated with critical enhancement set to zero.

4.2. Computer-program verification

For checking computer implementations of the correlation, we provide Table 11. The points are calculated with the tabulated temperatures and densities.

5. Conclusions

New wide-ranging correlations for the viscosity and thermal conductivity of *n*-undecane were developed based

TABLE 9. Viscosity and thermal conductivity values of *n*-undecane along the saturation line, calculated by the present scheme

T (K)	p (MPa)	ρ_{liq} (kg m^{-3})	ρ_{vap} (kg m^{-3})	η_{liq} (μPa s)	η_{vap} (μPa s)	λ_{liq} (mW m^{-1} K^{-1})	λ_{vap} (mW m^{-1} K^{-1})
300	6.639×10^{-5}	734.99	4.16×10^{-3}	1047	4.83	134.0	8.27
350	1.484×10^{-3}	696.87	8.00×10^{-2}	556.6	5.72	120.7	11.66
400	1.289×10^{-2}	657.80	6.16×10^{-1}	346.8	6.75	108.8	15.68
450	6.218×10^{-2}	616.19	2.73×10^{0}	234.2	8.03	98.31	20.26
500	2.051×10^{-1}	569.74	8.68×10^{0}	164.6	9.72	89.37	25.43
550	5.268×10^{-1}	514.09	2.30×10^{1}	116.5	12.10	82.19	31.71
600	1.150×10^{0}	436.84	5.92×10^{1}	78.7	16.16	77.25	41.98

on critically evaluated experimental data. The correlations are expressed in terms of temperature and density and are designed to be used with the equation of state of Aleksandrov *et al.*[23] that is valid from 247.606 K to 700 K, for densities up to 776.86 kg m^{-3}. The estimated uncertainty for the dilute-gas viscosity is 2.4%, and the estimated uncertainty for viscosity in the liquid phase for pressures up to 60 MPa over the temperature range 260 K–520 K is 5%. The correlation behaves in a smooth manner over the entire range of validity of the equation of state, but care should be taken when using the correlation outside of its validated range and uncertainties will be larger. The estimated uncertainty is 3% for the thermal conductivity of the low-density gas and 3% for the liquid over the temperature range from 284 K to 677 K at pressures up to 400 MPa. The thermal conductivity correlation behaves in a physically reasonable manner when extrapolated to the full range of the equation of state, but the uncertainties will be larger, especially in the critical region.

6. References

[1]M. J. Assael, J. A. M. Assael, M. L. Huber, R. A. Perkins, and Y. Takata, J. Phys. Chem. Ref. Data **40**, 033101 (2011).
[2]M. L. Huber, R. A. Perkins, D. G. Friend, J. V. Sengers, M. J. Assael, I. N. Metaxa, K. Miyagawa, R. Hellmann, and E. Vogel, J. Phys. Chem. Ref. Data **41**, 033102 (2012).
[3]M. J. Assael, I. A. Koini, K. D. Antoniadis, M. L. Huber, I. M. Abdulagatov, and R. A. Perkins, J. Phys. Chem. Ref. Data **41**, 023104 (2012).
[4]M. L. Huber, E. A. Sykioti, M. J. Assael, and R. A. Perkins, J. Phys. Chem. Ref. Data **45**, 013102 (2016).
[5]M. J. Assael, S. K. Mylona, M. L. Huber, and R. A. Perkins, J. Phys. Chem. Ref. Data **41**, 023101 (2012).
[6]M. J. Assael, E. K. Michailidou, M. L. Huber, and R. A. Perkins, J. Phys. Chem. Ref. Data **41**, 043102 (2012).
[7]C.-M. Vassiliou, M. J. Assael, M. L. Huber, and R. A. Perkins, J. Phys. Chem. Ref. Data **44**, 033102 (2015).
[8]M. J. Assael, S. K. Mylona, M. L. Huber, and R. A. Perkins, J. Phys. Chem. Ref. Data **42**, 013106 (2013).
[9]A. Koutian, M. J. Assael, M. L. Huber, and R. A. Perkins, J. Phys. Chem. Ref. Data **46**, 013102 (2017).
[10]M. J. Assael, I. Bogdanou, S. K. Mylona, M. L. Huber, R. A. Perkins, and V. Vesovic, J. Phys. Chem. Ref. Data **42**, 023101 (2013).
[11]E. A. Sykioti, M. J. Assael, M. L. Huber, and R. A. Perkins, J. Phys. Chem. Ref. Data **42**, 043101 (2013).
[12]M. J. Assael, E. A. Sykioti, M. L. Huber, and R. A. Perkins, J. Phys. Chem. Ref. Data **42**, 023102 (2013).
[13]M. J. Assael, A. Koutian, M. L. Huber, and R. A. Perkins, J. Phys. Chem. Ref. Data **45**, 033104 (2016).
[14]S. K. Mylona, K. D. Antoniadis, M. J. Assael, M. L. Huber, and R. A. Perkins, J. Phys. Chem. Ref. Data **43**, 043104 (2014).
[15]M. L. Huber, R. A. Perkins, A. Laesecke, D. G. Friend, J. V. Sengers, M. J. Assael, I. N. Metaxa, E. Vogel, R. Mares, and K. Miyagawa, J. Phys. Chem. Ref. Data **38**, 101 (2009).
[16]E. K. Michailidou, M. J. Assael, M. L. Huber, and R. A. Perkins, J. Phys. Chem. Ref. Data **42**, 033104 (2013).
[17]E. K. Michailidou, M. J. Assael, M. L. Huber, I. M. Abdulagatov, and R. A. Perkins, J. Phys. Chem. Ref. Data **43**, 023103 (2014).
[18]S. Avgeri, M. J. Assael, M. L. Huber, and R. A. Perkins, J. Phys. Chem. Ref. Data **43**, 033103 (2014).
[19]S. Avgeri, M. J. Assael, M. L. Huber, and R. A. Perkins, J. Phys. Chem. Ref. Data **44**, 033101 (2015).
[20]R. A. Perkins, M. L. Huber, and M. J. Assael, J. Chem. Eng. Data **61**, 3286 (2016).
[21]C. M. Tsolakidou, M. J. Assael, M. L. Huber, and R. A. Perkins, J. Phys. Chem. Ref. Data **46**, 023103 (2017).
[22]M. L. Huber and M. J. Assael, Int. J. Refrig. **71**, 39 (2016).
[23]I. S. Aleksandrov, A. A. Gerasimov, and B. A. Grigor'evb, Therm. Eng. **58**, 691 (2011).
[24]M. J. Assael, M. L. V. Ramires, C. A. Nieto de Castro, and W. A. Wakeham, J. Phys. Chem. Ref. Data **19**, 113 (1990).
[25]D. G. Friend and J. C. Rainwater, Chem. Phys. Lett. **107**, 590 (1984).
[26]J. C. Rainwater and D. G. Friend, Phys. Rev. A **36**, 4062 (1987).
[27]E. Bich and E. Vogel, in *Transport Properties of Fluids: Their Correlation Prediction and Estimation* (Cambridge University Press, Cambridge, 1996), Chap. 5.2.
[28]G. A. Iglesias-Silva, A. Guzmán-López, G. Pérez-Durán, and M. Ramos-Estrada, J. Chem. Eng. Data **61**, 2682 (2016).
[29]L. Zhang, Y. Guo, H. Wei, F. Yang, W. Fang, and R. Lin, J. Chem. Eng. Data **55**, 4108 (2010).
[30]J. Wu, Z. Shan, and A. A. Asfour, Fluid Phase Equilib. **143**, 263 (1998).
[31]M. J. Assael and M. Papadaki, Int. J. Thermophys. **12**, 801 (1991).
[32]H. Bauer and G. Meerlender, Rheol. Acta **23**, 514 (1984).
[33]S. O. Guseinov and Y. M. Naziev, Neft. Gazov. Promst. **12**, 61 (1973).
[34]A. K. Doolittle and R. H. Peterson, J. Am. Chem. Soc. **73**, 2145 (1951).
[35]Y. L. Rastorguev and A. S. Keramidi, Neft. Gazov. Promst. **14**, 59 (1971).
[36]A. F. Shepard, A. L. Henne, and T. Midgley, J. Am. Chem. Soc. **53**, 1948 (1931).
[37]E. C. Bingham and H. J. Fornwalt, J. Rheol. **1**, 372 (1930).
[38]V. Diky, R. D. Chirico, M. Frenkel, A. Bazykeva, J. W. Magee, E. Paulechka, A. F. Kazakov, E. W. Lemmon, C. D. Muzny, A. Y. Smolyanitsky, S. Townsend, and K. Kroenlein, NIST Standard Reference Database 103b, Thermo Data Engine, v10.1, National Institute of Standards and Technology, Gaithersburg, MD, 2016.
[39]N. Riesco and V. Vesovic, Fluid Phase Equilib. **425**, 385 (2016).
[40]G. C. Maitland, M. Rigby, E. B. Smith, and W. A. Wakeham, *Intermolecular Forces: Their Origin and Determination* (Clarendon, Oxford, 1981).
[41]EUREQA Formulize v.098.1 (Nutonian, Inc., Cambridge, MA, USA, 2012). Certain commercial products are identified in this paper to adequately specify the procedures used. Such identification does not imply recommendation or endorsement by the National Institute of Standards and Technology, nor does it imply that the products identified are necessarily the best available for that purpose.
[42]M. J. Assael, J. H. Dymond, M. Papadaki, and P. M. Patterson, Int. J. Thermophys. **13**, 269 (1992).
[43]Y. Wada, Y. Nagasaka, and A. Nagashima, Int. J. Thermophys. **6**, 251 (1985).
[44]J. C. G. Calado, J. M. N. A. Fareleira, C. A. Nieto de Castro, and W. A. Wakeham, Int. J. Thermophys. **4**, 193 (1983).
[45]J. Menashe and W. A. Wakeham, Ber. Bunsenges. Phys. Chem. **86**, 541 (1982).
[46]R. A. Mustafaev, Teplofiz. Vys. Temp. **12**, 772 (1974).
[47]R. A. Mustafaev, Izv. vyssh.ucheb. Zaved. Energ. **15**, 77 (1972).
[48]A. A. Tarzimanov and V. E. Mashirov, Teplofiz. Svoistva Veshchestv Mater **2**, 240 (1970).
[49]G. K. Mukhamedzyanov, A. G. Usmanov, and A. A. Tarzimanov, Izv. vyssh. ucheb. Zaved. Neft Gaz **9**, 75 (1963).
[50]Y. M. Naziev and M. A. Aliev, Izv. vyssh. ucheb. Zaved. Neft Gaz **16**, 73 (1973).
[51]R. W. Powell and H. Groot, Int. J. Heat Mass Transfer **15**, 360 (1972).
[52]A. K. Abas-Zade and K. D. Guseinov, Khim. Tekhn. Topl. i Masel **11**, 54 (1966).
[53]A. G. Akhmedov, Azerb. Neft. Khoz. **42**, 41 (1963).
[54]R. Hellmann, E. Bich, E. Vogel, and V. Vesovic, J. Chem. Eng. Data **57**, 1312 (2012).
[55]F. R. W. McCourt, J. J. M. Beenakker, W. E. Köhler, and I. Kučšer, *Non-equilibrium Phenomena in Polyatomic Gases* (Clarendon Press, Oxford, 1990).
[56]B. J. Thijsse, G. W. Thooft, D. A. Coombe, H. F. P. Knaap, and J. J. M. Beenakker, Physica A **98**, 307 (1979).
[57]J. Millat, V. Vesovic, and W. A. Wakeham, Physica A **148**, 153 (1988).
[58]S. Bock, E. Bich, E. Vogel, A. S. Dickinson, and V. Vesovic, J. Chem. Phys. **120**, 7987 (2004).

[59]R. Hellmann, E. Bich, E. Vogel, A. S. Dickinson, and V. Vesovic, J. Chem. Phys. **130**, 124309 (2009).
[60]R. Hellmann, E. Bich, E. Vogel, and V. Vesovic, Phys. Chem. Chem. Phys. **13**, 13749 (2011).
[61]G. A. Olchowy and J. V. Sengers, Phys. Rev. Lett. **61**, 15 (1988).
[62]R. Mostert, H. R. van den Berg, P. S. van der Gulik, and J. V. Sengers, J. Chem. Phys. **92**, 5454 (1990).
[63]R. A. Perkins, H. M. Roder, D. G. Friend, and C. A. Nieto de Castro, Physica A **173**, 332 (1991).
[64]P. T. Boggs, R. H. Byrd, J. E. Rogers, and R. B. Schnabel, ODRPACK, Software for Orthogonal Distance Regression, NISTIR 4834, v2.013, National Institute of Standards and Technology, Gaithersburg, MD, 1992.
[65]G. A. Olchowy and J. V. Sengers, Int. J. Thermophys. **10**, 417 (1989).
[66]R. A. Perkins, J. V. Sengers, I. M. Abdulagatov, and M. L. Huber, Int. J. Thermophys. **34**, 191 (2013).
[67]V. Vesovic, W. A. Wakeham, G. A. Olchowy, J. V. Sengers, J. T. R. Watson, and J. Millat, J. Phys. Chem. Ref. Data **19**, 763 (1990).